EFFECT OF ELLIPTIC OR CIRCULAR HOLES ON THE STRESS DISTRIBUTION IN PLATES OF WOOD OR PLYWOOD CONSIDERED AS ORTHOTROPIC MATERIALS

Information Revied and Reaffirmed

March 1956

No. 1510

FOREST PRODUCTS LABORATORY
MADISON 5, WISCONSIN

UNITED STATES DEPARTMENT OF AGRICULTURE
FOREST SERVICE
In Cooperation with the University of Wisconsin

EFFECT OF ELLIPTIC OR CIRCULAR HOLES ON THE STRESS DISTRIBUTION IN PLATES OF WOOD OR PLYWOOD CONSIDERED AS ORTHOTROPIC MATERIALS[1]

By

Forest Products Laboratory,[2] Forest Service
U. S. Department of Agiculture

- - - - -

Abstract

This is a mathematical analysis of the stress distribution existing near a hole in a wood or plywood plate subjected to tension, as, for example, near holes in the tension flanges of wood box beams. It is assumed that the strains are small and remain within the proportional. limit. In this analysis a large, rectangular, orthotropic plate with a small, elliptic hole at the center is subjected to a uniform tension along two opposite edger. By taking equal axes for the elliptic hole, the theoretical stress distribution in the neighborhood of a circular hole is obtained. The analysis shows that for a circular hole in a plain-sawn plate of Sitka spruce a maximum tensile stress of 5.84S is attained, S being the uniform tension applied in the direction of the grain. This maximum stress occurs on the edge of the circular hole at the ends of the diameter parpendicular to the direction of the uniform tension. Although this stress concentration may be greater than that found in isotropic materials, it is much more sharply localized and is relieved by plastic flow when the stress exceeds the proportional limit. For the reader who does not wish to follow the mathematical details of this report, the formula for computing this maximum stress for wood or plywood and an explanation of the constants involved is given in the appendix. The formula has not

---

[1]This progress report was originally preparted by the Forest Products Laboratory in 1944.

[2]Maintained at Madison, Wis., in cooperation with the University of Wisconsin.

been confirmed by an extensive series of tests, but it was found to be in reasonably satisfactory agreement with the only test made. It is also demonstrated that for the Sitka spruce plate mentioned the maximum shear stress attained is 0.71S (fig. 5). The stress function from which these formulas for the orthotropic case are obtained is shown to reduce to the well-known stress function for the isotropic case.

Introduction

An orthotropic material possesses three planes of elastic symmetry at right angles to each other. If from such a material a flat plate is cut parallel to a plane of symmetry, it will have two perpendicular axes of symmetry in the plane of the plate. In the discussion that follows, a large rectangular orthotropic plate of this type with its edges parallel to the axes of symmetry and with a small hole at its center will be considered. A uniform tension S will be taken to act on two opposite edges of the plate as shown in figure 1, and the resulting stress distribution will be obtained. Throughout the report it is assumed that the strains are small and remain within the limits of "perfect elasticity."

The solution is first derived for an elliptic hole with major and minor axes coinciding with the axes of symmetry. By taking the major and minor axes equal, the solution for a circular hole is obtained. For the orthotropic plate, the solution for the circular hole is but slightly more simple than that for the elliptic hole. This is different from the corresponding problem for the isotropic plate.[3] The stress-strain distribution in the neighborhood of the circular hole is notably different in an orthotropic plate than in an isotropic plate as the concentration may be considerably higher and of a more localized character for the orthotropic than for the isotropic plate. Thus in a plate of plain-sawn Sitka spruce with a uniform tension acting in the grain direction, the greatest stress component at the edge of the hole decreases rapidly to one-half of its maximum value in a radial distance of less than one-tenth of the radius. For the isotropic plate the corresponding stress component decreases to one-half of its maximum value in a radial distance larger than one-half of the radius from the edge of the hole.

[3] Timoshenko, S. Theory of Elasticity.

The Effect of Eliptic or Circular Holes on the Stress Distribution in a Wood Plate

The components of stress and strain in a plate under plane stress are connected by the following relations[4] if the axes of x and y are taken as the axes of elastic symmetry of the orthotropic plate:

$$\left.\begin{aligned} e_{xx} &= \frac{1}{E_x} X_x - \frac{\sigma_{yx}}{E_y} Y_y \\ e_{yy} &= -\frac{\sigma_{xy}}{E_x} X_x + \frac{1}{E_y} Y_y \\ e_{xy} &= \frac{1}{\mu_{xy}} X_y \end{aligned}\right\} \qquad (1)$$

In these equations E_x and E_y are Young's moduli in the x- and y-directions, respectively. Poisson's ratio σ_{xy} is the ratio of the contraction parallel to the y-axis to the extension parallel to the x-axis associated with a tension parallel. to the x-axis and similarly for σ_{yx}. The quantity μ_{xy} is the modulus of rigidity associated with the directions of x and y.

Since the equations of equilibrium are deduced with no reference to the law connecting stresses and strainns, they will be satisfied by a stress function F such that

$$X_x = \frac{\partial^2 F}{\partial y^2}, \qquad Y_y = \frac{\partial^2 F}{\partial x^2}, \qquad X_y = -\frac{\partial^2 F}{\partial x \partial y} \qquad (2)$$

---

[4] March, H.W., Stress-Strain Relations in Wood and Plywood Considered as Orthotropic Materials, U. S. Forest Products Laboratory Report No. 1503.

Substituting (2) in (1) and then making use of the compatibility equation

$$\frac{\partial^2 e_{xx}}{\partial y^2} + \frac{\partial^2 e_{yy}}{\partial x^2} = \frac{\partial^2 e_{xy}}{\partial x \partial y}$$

the following differential equation, satisfied by the stress function F, is obtained:

$$\frac{1}{E_y} \frac{\partial^4 F}{\partial x^4} + \left(\frac{1}{\mu_{xy}} - 2 \frac{\sigma_{xy}}{E_x}\right) \frac{\partial^4 F}{\partial x^2 \partial y^2} + \frac{1}{E_x} \frac{\partial^4 F}{\partial y^4} = 0 \tag{3}$$

In deriving (3), the relation[4]

$$\frac{\sigma_{xy}}{E_x} = \frac{\sigma_{yx}}{E_y} \tag{4}$$

has been used.

It is convenient to rewrite equation (3) as[5]

$$\frac{\partial^4 F}{\partial x^4} + 2\kappa \frac{\partial^4 F}{\partial x^2 \partial \eta^2} + \frac{\partial^4 F}{\partial \eta^4} = 0 \tag{5}$$

where

$$\kappa = \frac{\sqrt{E_x E_y}}{2} \left(\frac{1}{\mu_{xy}} - \frac{2\sigma_{xy}}{E_x}\right) \tag{6}$$

by making the substitution

$$\eta = \epsilon y \tag{7}$$

---

[5] March, H, W., Flat Plates of Plywood Under Uniform or Concentrated Loads, U. S. Forest Products Laboratory Report No. 1312.

where

$$\epsilon = \sqrt[4]{\frac{E_x}{E_y}} \tag{8}$$

Substituting $\underline{F} = \underline{F(x + \nu\eta)}$ in (5) leads to the following equation for $\underline{\nu}$:

$$\nu^4 + 2\kappa\nu^2 + 1 = 0 \tag{9}$$

or

$$\nu^2 = -\kappa \pm \sqrt{\kappa^2 - 1} \quad . \tag{10}$$

Now let[6]

$$\kappa = \cosh\phi \tag{11}$$

then

$$\nu^2 = -\cosh\phi \pm \sqrt{\cosh^2\phi - 1}$$

$$= -\cosh\phi \pm \sinh\phi$$

$$= -\frac{e^{\phi} + e^{-\phi}}{2} \pm \frac{e^{\phi} - e^{-\phi}}{2} = -e^{\phi} \text{ or } -e^{-\phi} \quad .$$

[6] For wood or plywood, $\underline{k}$ as defined here is probably always greater than 1.

Hence, the roots of equation (9) are

$$\nu_1 = ie^{\phi/2}, \quad \nu_2 = ie^{-\phi/2}, \quad \nu_3 = -ie^{\phi/2}, \quad \nu_4 = -ie^{-\phi/2}$$

Equation (5) may now be written as

$$\left(\frac{\partial^2}{\partial x^2} + \alpha^2 \frac{\partial^2}{\partial \eta^2}\right)\left(\frac{\partial^2}{\partial x^2} + \beta^2 \frac{\partial^2}{\partial \eta^2}\right) F = 0 \tag{12}$$

where

$$\alpha^2 = e^{\phi}, \qquad \beta^2 = e^{-\phi} \tag{13}$$

The solution of equation (13) is facilitated by taking F of the form

$$F = R\left[F_1(x + i\alpha\eta) + F_2(x + i\beta\eta)\right] + F_o(x, \eta) \tag{14}$$

where

$$\alpha = e^{\phi/2} = \sqrt{\kappa + \sqrt{\kappa^2 - 1}}, \qquad \beta = e^{-\phi/2} = \sqrt{\kappa - \sqrt{\kappa^2 - 1}},$$

$$i = \sqrt{-1} \tag{15}$$

$F_o(x, \eta)$ is any particular solution of (12), and the letter R means that the real part of the expression in the bracket is to be taken. That (14) is a solution of (12) is easily established by direct substitution. Equations (12) and (14) hold for the stress function associated with any elastic problem of plane stress in an orthotropic plate with x- and y- axes chosen as described here.

A suitable choice of F for the problem discussed is

$$F = R\left\{\frac{A}{2\gamma_1^2}\left[\frac{1}{2}(z_1 - w_1)^2 + \gamma_1^2 \log(z_1 + w_1)\right] + \frac{B}{2\gamma_2^2}\left[\frac{1}{2}(z_2 - w_2)^2 + \gamma_2^2 \log(z_2 + w_2)\right]\right\} + \frac{S\eta^2}{2\epsilon^2} \tag{16}$$

where

$$z_1 = x + i\alpha\eta\ , \qquad z_2 = x + i\beta\eta\ ,$$

$$w_1 = \sqrt{z_1^2 - \gamma_1^2}\ , \qquad w_2 = \sqrt{z_2^2 - \gamma_2^2}\ . \tag{17}$$

$$\gamma_1^2 = a^2 - \alpha^2\epsilon^2 b^2\ , \qquad \gamma_2^2 = a^2 - \beta^2\epsilon^2 b^2\ , \tag{18}$$

the boundary of the hole (fig. 1) is given by

$$x = a\cos\theta\ , \qquad \eta = \epsilon y = \epsilon b \sin\theta\ , \tag{19}$$

and S is the uniform tension applied at the ends of the plate.

In order that the stresses may be single-valued, the square roots in (17) are to be chosen so that the following relations always hold:

$$\left|z_1 + w_1\right| \geqq \left|\gamma_1\right|, \qquad \left|z_2 + w_2\right| \geqq \left|\gamma_2\right|.$$

Then

$$\frac{\partial F}{\partial x} = R\left\{A\left[\frac{1}{z_1 + w_1}\right] + B\left[\frac{1}{z_2 + w_2}\right]\right\} \tag{20}$$

and

$$\frac{\partial F}{\partial \eta} = R\left\{A\left[\frac{\alpha i}{z_1 + w_1}\right] + B\left[\frac{\beta i}{z_2 + w_2}\right]\right\} + \frac{S\eta}{\epsilon^2} \quad . \tag{21}$$

On the boundary of the hole x and η are given by (19), so that

$$z_1 + w_1 = a \cos\theta + i\alpha\epsilon\, b \sin\theta$$

$$+ \sqrt{a^2 \cos^2\theta + 2i\alpha\epsilon\, ab \cos\theta \sin\theta - \alpha^2\epsilon^2 b^2 \sin^2\theta - a^2 + \alpha^2\epsilon^2 b^2} \; ,$$

$$= a \cos\theta + i\alpha\epsilon\, b \sin\theta + (\alpha\epsilon b \cos\theta + ia \sin\theta) \tag{22}$$

$$= (a + \alpha\epsilon b)\, e^{i\theta} \quad . \tag{23}$$

Similarly, on the edge of the hole

$$z_2 + w_2 = (a + \beta\epsilon b)\, e^{i\theta} \quad . \tag{24}$$

Consider the boundary of the hole in figure 2, and orient the positive direction of the normal v and of the tangent τ relative to one another in a way similar to the orientation of the x- and y-axis, respectively.

Let X_ν ds and Y_ν ds represent and x- and y-components of the force per unit thickness of the plate, acting on the element of arc ds of the boundary from the positive side indicated by the direction of positive ν. Then

$$X_\nu = X_x \cos(x, \nu) + X_y \cos(y, \nu) \quad ,$$

$$= \frac{\partial^2 F}{\partial y^2} \cos(x, \nu) - \frac{\partial^2 F}{\partial x \partial y} \cos(y, \nu) \quad .$$

$$Y_\nu = X_y \cos(x, \nu) + Y_y \cos(y, \nu) \quad ,$$

$$= -\frac{\partial^2 F}{\partial x \partial y} \cos(x, \nu) + \frac{\partial^2 F}{\partial x^2} \cos(y, \nu) \quad .$$

But

$$\cos(x, \nu) = \cos(y, \tau) = \frac{dy}{ds} \quad ,$$

$$\cos(y, \nu) = -\cos(x, \tau) = -\frac{dx}{ds} \tag{25}$$

so that

$$X_\nu = \frac{\partial^2 F}{\partial y^2} \frac{dy}{ds} + \frac{\partial^2 F}{\partial x \partial y} \frac{dx}{ds} = \frac{d}{ds} \left(\frac{\partial F}{\partial y}\right)$$

$$Y_\nu = -\frac{\partial^2 F}{\partial x \partial y} \frac{dy}{ds} - \frac{\partial^2 F}{\partial x^2} \frac{dx}{ds} = -\frac{d}{ds} \left(\frac{\partial F}{\partial x}\right) \quad . \tag{26}$$

Equations (26) for a boundary on which no stresses act take the form

$$\frac{d}{ds}\left(\frac{\partial F}{\partial y}\right) = 0 \quad , \qquad \frac{d}{ds}\left(\frac{\partial F}{\partial x}\right) = 0 \quad .$$

Hence, $\frac{\partial F}{\partial x}$ and $\frac{\partial F}{\partial y}$ are constant along a free boundry.

Then, on the boundary of the hole,

$$\frac{\partial F}{\partial x} = c_1 \quad , \qquad \frac{\partial F}{\partial y} = \epsilon \frac{\partial F}{\partial \eta} = c_2 \quad . \tag{27}$$

Substituting (23) and (24) in (20) and (21), it follows from (27) that

$$R \left[A \frac{e^{-i\theta}}{a + \alpha\epsilon b} + B \frac{e^{-i\theta}}{a + \beta\epsilon b} \right] = c_1 \quad ,$$

and

$$R \left[A \frac{\alpha i e^{-i\theta}}{a + \alpha\epsilon b} + B \frac{\beta i e^{-i\epsilon}}{a + \beta\epsilon b} \right] + \frac{S\epsilon b \sin\theta}{\epsilon^2} = \frac{c_2}{\epsilon} \quad . \tag{28}$$

Taking the real parts

$$\left[\frac{A}{a + \alpha\epsilon b} + \frac{B}{a + \beta\epsilon b} \right] \cos\theta = c_1 \quad ,$$

$$\left[\frac{A\alpha}{a + \alpha\epsilon b} + \frac{B\beta}{a + \beta\epsilon b} + \frac{Sb}{\epsilon} \right] \sin\theta = \frac{c_2}{\epsilon} \quad . \tag{29}$$

These equations must be satisfied for any value of $\underline{\theta}$, hence

$$\frac{A}{a + \alpha\epsilon b} + \frac{B}{a + \beta\epsilon b} = 0 \quad , \qquad c_1 = 0 \quad ,$$

and

$$\frac{A\alpha}{a + \alpha\epsilon b} + \frac{B\beta}{a + \beta\epsilon b} + \frac{Sb}{\epsilon} = 0 \quad , \qquad c_2 = 0 \quad .$$

Therefore,

$$A = -\frac{Sb\,(a + \alpha\epsilon b)}{\epsilon\,(\alpha - \beta)} \quad ,$$

$$B = \frac{Sb\,(a + \beta\epsilon b)}{\epsilon\,(\alpha - \beta)} \quad . \tag{30}$$

By using equations (30), the stress components are found to be

$$\frac{\partial^2 F}{\partial x^2} = Y_y = R\left\{\frac{Sb}{\epsilon\,(\alpha - \beta)}\left[\frac{(a + \alpha\epsilon b)}{w_1\,(z_1 + w_1)} - \frac{(a + \beta\epsilon b)}{w_2\,(z_2 + w_2)}\right]\right\} \tag{31}$$

$$\epsilon^2\,\frac{\partial^2 F}{\partial y^2} = X_x = R\left\{\frac{S\epsilon b}{(\alpha - \beta)}\left[\frac{-\alpha^2(a + \alpha\epsilon b)}{w_1\,(z_1 + w_1)} + \frac{\beta^2(a + \beta\epsilon b)}{w_2\,(z_2 + w_2)}\right]\right\} + S \tag{32}$$

$$-\epsilon\,\frac{\partial^2 F}{\partial x \partial \eta} = X_y = R\left\{\frac{Sb}{(\alpha - \beta)}\left[\frac{-\alpha i(a + \alpha\epsilon b)}{w_1\,(z_1 + w_1)} + \frac{\beta i(a + \beta\epsilon b)}{w_2\,(z_2 + w_2)}\right]\right\} \quad . \tag{33}$$

To obtain the stress components for a circular hole, it is only necessary to let $\underline{b} = \underline{a}$ in equations (31), (32), and (33). Then

$$Y_y = R\left\{\frac{Sa^2}{\epsilon(\alpha - \beta)}\left[\frac{(1 + \alpha\epsilon)}{w_1'(z_1 + w_1')} - \frac{(1 + \beta\epsilon)}{w_2'(z_2 + w_2')}\right]\right\} \tag{34}$$

$$X_x = R\left\{\frac{Sa^2\epsilon}{\alpha - \beta}\left[\frac{-\alpha^2(1 + \alpha\epsilon)}{w_1'(z_1 + w_1')} + \frac{\beta^2(1 + \beta\epsilon)}{w_2'(z_2 + w_2')}\right]\right\} + S \tag{35}$$

$$X_y = R\left\{\frac{Sa^2}{\alpha - \beta}\left[\frac{-\alpha i(1 + \alpha\epsilon)}{w_1'(z_1 + w_1')} + \frac{\beta i(1 + \beta\epsilon)}{w_2'(z_2 + w_2')}\right]\right\} \tag{36}$$

where

$$w_1' = \sqrt{z_1^2 - a^2(1 - \alpha^2\epsilon^2)}\ , \qquad w_2' = \sqrt{z_2^2 - a^2(1 - \beta^2\epsilon^2)}\ , \tag{37}$$

Expressions (31), (32), (33) are complicated and do not permit easy computation of the numerical values of the stresses. The most important information they contain is, of course, in the neighborhood of the hole.

Stresses at the Edge of the Hole

From equations (22), (23), and (24), it is found that over the edge of the elliptic hole

$$Y_y = R\left\{\frac{Sbe^{-i\theta}}{\epsilon(\alpha - \beta)}\left[\frac{1}{\alpha\epsilon b\cos\theta + ia\sin\theta} - \frac{1}{\beta\epsilon b\cos\theta + ia\sin\theta}\right]\right\}, \tag{38}$$

$$X_x = R\left\{\frac{S\epsilon be^{-i\theta}}{(\alpha - \beta)}\left[\frac{-\alpha^2}{\alpha\epsilon b\cos\theta + ia\sin\theta} + \frac{\beta^2}{\beta\epsilon b\cos\theta + ia\sin\theta}\right]\right\} + S\ , \tag{39}$$

$$X_y = R\left\{\frac{Sbe^{-i\theta}}{(\alpha - \beta)}\left[\frac{-\alpha i}{\alpha\epsilon b \cos\theta + ia \sin\theta} + \frac{\beta i}{\beta\epsilon b \cos\theta + ia \sin\theta}\right]\right\} . \tag{40}$$

Since, by (15) $\underline{\alpha\beta} = 1$, the real parts are given by

$$Y_y = \frac{T_\tau}{a^2 \sin^2\theta + b^2 \cos^2\theta} b^2 \cos^2\theta \quad , \tag{41}$$

$$X_x = \frac{T_\tau}{a^2 \sin^2\theta + b^2 \cos^2\theta} a^2 \sin^2\theta \quad , \tag{42}$$

$$X_y = \frac{-T_\tau}{a^2 \sin^2\theta + b^2 \cos^2\theta} ab \sin\theta \cos\theta \quad . \tag{43}$$

where

$$T_\tau = \frac{S(a^2 \sin^2\theta + b^2 \cos^2\theta)\left[-\epsilon^2 b^2 \cos^2\theta + a(\alpha\epsilon b + \beta\epsilon b + a)\sin^2\theta\right]}{(\alpha^2\epsilon^2 b^2 \cos^2\theta + a^2 \sin^2\theta)(\beta^2\epsilon^2 b^2 \cos^2\theta + a^2 \sin^2\theta)} \quad . \tag{44}$$

It is of interest to refer these stresses at the edge of the hole to a pair of axes at right angles to each other having the directions of the normal $\underline{\nu}$ and the tangent τ, respectively (fig. 2). In this coordinate system, the shearing stress and the tension (or compression) in the $\underline{\nu}$-direction must vanish, as this is required by the boundary conditions. It is readily shown that $\underline{T_\tau}$ of equation (44) is the tension (or compression) in the tangential direction. The component of direct stress in the tangential direction is given by

$$X_x \cos^2(x, \tau) + Y_y \cos^2(y, \tau) + 2X_y \cos(x, \tau)\cos(y, \tau) \quad .$$

From (19) and (25), this becomes

$$\frac{X_x a^2 \sin^2 \theta + Y_y b^2 \cos^2 \theta - 2X_y ab \cos \theta \sin \theta}{a^2 \sin^2 \theta + b^2 \cos^2 \theta} .$$

Substituting from (41), (42), and (43), the tangential stress is found to be identical with T_t of equation (44). If $\varepsilon \geqq 1$, it follows that at the end of the axis perpendicular to the direction of the tension, that is for $\theta = 90°$ (fig. 1), T_τ attains its maximum value, while at the end of the axis parallel to the tension, that is $\theta = 0°$, T_τ attains its minimum value. Then

$$T_\tau \text{ (max.)} = \frac{S}{a} (\alpha\varepsilon b + \beta\varepsilon b + a) , \tag{45a}$$

$$T_\tau \text{ (min.)} = - \frac{S}{\varepsilon^2} . \tag{46}$$

For an isotropic material, it follows from (6), (8), (11), and (15) that $\alpha = \beta = \varepsilon = 1$. Introducing these values, (45a) and (46) become $S(\frac{2b}{a} + 1)$ and $-S$, respectively, as in the isotropic case.[3]

Equation (45a) gives the tension at C (fig. 1) the highest stress occurring in the plate. Numerical values of this stress will be computed in the two cases $\frac{b}{a} = 50$ and $\frac{b}{a} = \frac{1}{50}$ for a plain-sawn plate of Sitka spruce whose elastic moduli are given in table 1. The grain direction is taken parallel to the line $\theta = 0°$.

When $\frac{b}{a} = 50$, the tension at C (fig. 1) is 243.2 times the mean tension.

When $\frac{b}{a} = \frac{1}{50}$, the tension at C (fig. 1) is 1.097 times the mean tension.

The ellipse when $\frac{b}{a} = 50$ would appear as a straight crack perpendicular to the grain which might be approximated by a break in the fibers, such as a compression failure. A very small tension applied to the plate across the crack would set up a tension at the ends of very high intensity. If this high tension at the ends caused the crack to tear, the increase in length would exaggerate the stress still further, and the crack would continue to spread.

When $\frac{b}{a} = \frac{1}{50}$ the ellipse would appear as a straight crack running in the direction of the grain or of the tension. Such a crack does not produce great local stress, a conclusion which is almost self-evident.

If the hole is circular ($\frac{b}{a} = 1$), equations (41), (42), (43), and (44) reduce to

$$Y_y = T'_T \cos^2\theta \quad , \quad X_x = T'_T \sin^2\theta \quad , \quad X_y = -T'_T \sin\theta\cos\theta \ ,$$

where

$$T'_T = \frac{S\left[-\epsilon^2\cos^2\theta + (\alpha\epsilon + \beta\epsilon + 1)\sin^2\theta\right]}{(\alpha^2\epsilon^2\cos^2\theta + \sin^2\theta)(\beta^2\epsilon^2\cos^2\theta + \sin^2\theta)} \ .$$

The stress at the end of the diameter perpendicular to the direction of the tension for a circular hole is given by

$$T'_{T\,(max.)} = S\,(\alpha\epsilon + \beta\epsilon + 1) \ . \tag{45b}$$

For an isotropic plate ($\alpha = \beta = \epsilon = 1$) this reduces to $3S$, as is well known,[3] but for a wood plate, equation (45b) may give a stress as high as $5.84S$ (fig. 8).

Experimental Verification of Maximum Stress

This maximum stress was experimentally verified by compressing a quarter-sawn yellow-poplar board containing a circular hole. The dimensions of the board and hole and the position of the 1/8-inch metalectric strain gages at P on the circumference of the hole and at Q at some distance from the hole are shown in figure 3. The gage measuring the maximum strain at P was placed inside the hole as shown in figure 3, since the maximum strain occurs just on the edge of the hole and dies off rapidly in the radial direction. The gage at Q is placed as far from the hole as is feasible for the specimen used. The gage length was assumed short enough to give a close approximation to the actual strain at the end of the diameter. Table 2 gives the experimental and the theoretical values of the strains at pints P and Q of figure 3. The theoretical strains were computed in terms of S from the stresses given by formulas (35) and (45b) using the elastic moduli of the yellow-poplar plate. These moduli were obtained from coupons cut from the specimen and are given in table 1.

The experimental value of the ratio of the strain at P to the strain at Q (fig. 3) is about 16 percent less than the theoretical one. This difference is not considered serious as the mathematical analysis was based on the assumption that the dimensions of the plate were large as compared to the dimensions of the hole. Also the impossibility of measuring strain at a point acted to decrease the apparent ratio. It is important to note that the experimental ratio is considerably higher than the corresponding ratio existing for a circular hole in an isotropic plate.

Shear Stress at the Edge of the Hole

The expression (43) for the shear component at the edge of the hole is highly important when considering holes in wood plates. When the uniform tension is parrallel to the grain direction, this shear acts in the same direction, and its distribution may indicate where failure caused by shear will take place if the uniform tension is sufficiently high. This statement has experimental verification when $\frac{b}{a} = 1$, as this type of failure occurred in wood box beams with small circular holes in their tension flanges tested at the U. S. Forest Products Laboratory (see fig. 4), The failure occurred in the vicinity of the point of maximum shear, which occurs theoretically, as shown in figure 5, at about $\theta = 78°$. The shear stress at the edge of the hole was evaluated numerically when $\frac{b}{a} = 1$ for a plain-sawn plate of Sitka spruce whose elastic moduli are given in

table 1. The results are given in table 3 for values of $\underline{\theta}$ between 0° and 90° when the line $\underline{\theta} = 0°$ is taken to be parallel to the grain of the wood. The shear at other points on the circle may be easily filled in from the given values. Figure 5 illustrates the variation of $\underline{X_y}$ over the edge of the hole for spruce and an isotropic material.

Stress Components at Points Along the x- and y-Axes

Simple expressions will now be obtained for the stress components at points along the x- and y-axes.

Writing equation (31) as

$$Y_y = R\left\{\frac{Sb}{\epsilon(\alpha - \beta)}\left[\frac{(a + \alpha\epsilon b)(z_1 - w_1)}{w_1(z_1 + w_1)(z_1 - w_1)} - \frac{(a + \beta\epsilon b)(z_2 - w_2)}{w_2(z_2 + w_2)(z_2 - w_2)}\right]\right\}$$

and performing similar operations on equation (32) and (33), it is found that

$$Y_y = R\left\{\frac{Sb}{\epsilon(\alpha - \beta)}\left[\frac{1}{a - \alpha\epsilon b}\left(\frac{z_1}{w_1} - 1\right) + \frac{1}{a - \beta\epsilon b}\left(\frac{z_2}{w_2} - 1\right)\right]\right\} ,$$

$$X_x = R\left\{\frac{S\epsilon b}{(\alpha - \beta)}\left[\frac{-\alpha^2}{a - \alpha\epsilon b}\left(\frac{z_1}{w_1} - 1\right) + \frac{\beta^2}{a - \beta\epsilon b}\left(\frac{z_2}{w_2} - 1\right)\right]\right\} + S , \quad (47)$$

$$X_y = R\left\{\frac{Sb}{(\alpha - \beta)}\left[\frac{-\alpha i}{a - \alpha\epsilon b}\left(\frac{z_1}{w_1} - 1\right) + \frac{\beta i}{a - \beta\epsilon b}\left(\frac{z_2}{w_2} - 1\right)\right]\right\} .$$

These equations can be reduced considerably when $\underline{x} = 0$ or $\underline{y} = 0$. The resulting equations then readily show how the stress concentration dies off with increasing distance from the hole.

For $\underline{x} = 0$, $\underline{y} \geqq \underline{a}$ it follows that

$$Y_y = \frac{Sb}{\epsilon(\alpha - \beta)}\left[\frac{1}{a - \alpha\epsilon b}\left(\frac{\alpha\epsilon y}{\sqrt{\alpha^2\epsilon^2 y^2 + \gamma_1^2}} - 1\right) - \frac{1}{a - \beta\epsilon b}\left(\frac{\beta\epsilon y}{\sqrt{\beta^2\epsilon^2 y^2 + \gamma_2^2}} - 1\right)\right]$$

$$X_x = \frac{S\epsilon b}{(\alpha - \beta)}\left[\frac{-\alpha^2}{a - \alpha\epsilon b}\left(\frac{\alpha\epsilon y}{\sqrt{\alpha^2\epsilon^2 y^2 + \gamma_1^2}} - 1\right) + \frac{\beta^2}{a - \beta\epsilon b}\left(\frac{\beta\epsilon y}{\sqrt{\beta^2\epsilon^2 y^2 + \gamma_2^2}} - 1\right)\right] + S \qquad (48)$$

$$X_y = 0$$

and for $\underline{y} = 0$, $\underline{x} \geqq a$

$$Y_y = \frac{S\epsilon b}{\epsilon(\alpha - \beta)}\left[\frac{-\alpha^2}{a - \alpha\epsilon b}\left(\frac{x}{\sqrt{x^2 - \gamma_1^2}} - 1\right) - \frac{1}{a - \beta\epsilon b}\left(\frac{x}{\sqrt{x^2 - \gamma_2^2}} - 1\right)\right]$$

$$X_x = \frac{Sb}{(\alpha - \beta)}\left[\frac{1}{a - \alpha\epsilon b}\left(\frac{x}{\sqrt{x^2 - \gamma_1^2}} - 1\right) + \frac{\beta^2}{a - \beta\epsilon b}\left(\frac{x}{\sqrt{x^2 - \gamma_2^2}} - 1\right)\right] + S \qquad (49)$$

$$X_y = 0 \ .$$

When $\frac{\underline{b}}{\underline{a}} = 1$ the distances from the center of the hole may be expressed as multiples of the radius by writing $\underline{x}^1 = \frac{\underline{x}}{\underline{a}}$, $\underline{y}^1 = \frac{\underline{y}}{\underline{a}}$ in equations (48) and (49). Hence, the stress components at points along the positive $\underline{y}$-axis for a circular hole are given by

$$Y_y = \frac{S}{\epsilon(\alpha - \beta)} \left[\frac{1}{1 - \alpha\epsilon} \left(\frac{\alpha\epsilon y'}{\sqrt{\alpha^2\epsilon^2 (y'^2 - 1) + 1}} - 1 \right) - \frac{1}{1 - \beta\epsilon} \left(\frac{\beta\epsilon y'}{\sqrt{\beta^2\epsilon^2 (y'^2 - 1) + 1}} - 1 \right) \right]$$

$$X_x = \frac{S\epsilon}{(\alpha - \beta)} \left[\frac{-\alpha^2}{1 - \alpha\epsilon} \left(\frac{\alpha\epsilon y'}{\sqrt{(\alpha^2\epsilon^2 (y'^2 - 1) + 1}} - 1 \right) + \frac{\beta^2}{1 - \beta\epsilon} \left(\frac{\beta\epsilon y'}{\sqrt{\beta^2\epsilon^2 (y'^2 - 1) + 1}} - 1 \right) \right] + S \tag{50}$$

$$X_y = 0$$

and at points along the positive $\underline{x}$-axis

$$Y_y = \frac{S}{\epsilon(\alpha - \beta)} \left[\frac{1}{1 - \alpha\epsilon} \left(\frac{x'}{\sqrt{x'^2 - 1 + \alpha^2\epsilon^2}} - 1 \right) - \frac{1}{1 - \beta\epsilon} \left(\frac{x'}{\sqrt{x'^2 - 1 + \beta^2\epsilon^2}} - 1 \right) \right]$$

$$X_x = \frac{S\epsilon}{(\alpha - \beta)} \left[\frac{-\alpha^2}{1 - \alpha\epsilon} \left(\frac{x'}{\sqrt{x'^2 - 1 + \alpha^2\epsilon^2}} - 1 \right) + \frac{\beta^2}{1 - \beta\epsilon} \left(\frac{x'}{\sqrt{x'^2 - 1 + \beta^2\epsilon^2}} - 1 \right) \right] + S \tag{51}$$

$$X_y = 0 \quad .$$

Numerical values of the stress components $\underline{X_x}$ and $\underline{Y_y}$ at points along the $\underline{x}$- and $\underline{y}$-axis when $\frac{b}{a} = 1$ are given in tables 4 and 5 for a plain-sawn plate of Sitka spruce. The variation of these components is illustrated in figures 6, 7, 8, and 9, and the variation of the corresponding stress components for an isotropic material is also shown for comparison. It is evident from these figures that considerable differences may exist between the stress distribution developed in the orthotropic plate as compared to the isotropic plate. In particular, figure 8 shows that the maximum stress developed in the spruce plate is nearly twice the maximum stress developed in the isotropic plate.

Displacements in the Neighborhood of a Circular Hole

The expressions for the displacements in the neighborhood of a circular hole ($\frac{b}{a} = 1$) will now be obtained.

Substituting (34) and (35) in the first two equations of (1), it is found that

$$e_{xx} = \frac{\partial u}{\partial x} = R\left\{\frac{Sa^2\epsilon}{(\alpha - \beta)E_x}\left[\frac{-\alpha^2(1+\alpha\epsilon)}{w_1'(z_1+w_1')} + \frac{\beta^2(1+\beta\epsilon)}{w_2'(z_2+w_2')}\right] - \frac{Sa^2\sigma_{yx}}{\epsilon(\alpha-\beta)E_y}\left[\frac{(1+\alpha\epsilon)}{w_1'(z_1+w_1')} - \frac{(1+\beta\epsilon)}{w_2'(z_2+w_2')}\right]\right\} \frac{S}{E_x}$$

$$e_{yy} = \frac{\partial v}{\partial y} = R\left\{\frac{Sa^2}{\epsilon(\alpha-\beta)E_y}\left[\frac{(1+\alpha\epsilon)}{w_1'(z_1+w_1')} - \frac{(1+\beta\epsilon)}{w_2'(z_2+w_2')}\right] - \frac{Sa^2\epsilon\sigma_{xy}}{(\alpha-\beta)E_x}\left[\frac{-\alpha^2(1+\alpha\epsilon)}{w_1'(z_1+w_1')} + \frac{\beta^2(1+\alpha\epsilon)}{w_2'(z_2+w_2')}\right]\right\} - \frac{S\sigma_{xy}}{E_x} \tag{52}$$

Integration of equations (52), gives

$$u = R\left\{\frac{Sa^2}{(\alpha - \beta)}\left[\left(\frac{\epsilon\alpha^2}{E_x} + \frac{\sigma_{yx}}{\epsilon E_y}\right)\frac{(1+\alpha\epsilon)}{z_1 + w_1'} - \left(\frac{\epsilon\beta^2}{E_x} + \frac{\sigma_{yx}}{\epsilon E_y}\right)\frac{(1+\beta\epsilon)}{z_2 + w_2'}\right]\right\} + \frac{Sx}{E_x}$$

(53)

$$v = R\left\{\frac{Sa^2}{(\alpha - \beta)}\left[-\frac{1}{i\alpha\epsilon}\left(\frac{1}{\epsilon E_y} + \frac{\epsilon\alpha^2\sigma_{xy}}{E_x}\right)\frac{(1+\alpha\epsilon)}{z_1 + w_1'} + \frac{1}{i\beta\epsilon}\right.\right.$$

$$\left.\left.\times\left(\frac{1}{\epsilon E_y} + \frac{\epsilon\beta^2\sigma_{xy}}{E_x}\right)\frac{(1+\beta\epsilon)}{z_2 + w_2'}\right]\right\} - \frac{S\sigma_{xy}}{E_x}\,y \quad .$$

These are the actual displacements except for the addition of a linear function of y and a linear function of x to the expressions for u and v, respectively. This is easily shown by deriving the expression for $e_{xy} = \frac{\partial u}{\partial y} + \frac{\partial v}{\partial x}$ and comparing it with the expression $\frac{1}{\mu_{xy}} X_y$. These additive functions may be made to vanish by fixing the origin and eliminating rotation about the origin.

Next the real and imaginary parts of $(z_1 + w_1')^{-1}$ and of a similar expression for z_2 and w_2 will be found. To do this, it will be useful to write

$$\frac{1}{z_1 + w_1'} = \frac{z_1 - w_1'}{a^2(1 - \alpha^2\epsilon^2)} \quad .$$

Let

$$w_1' = \sqrt{R_1}\ (\cos\Psi_1 + i\sin\Psi_1) \tag{54}$$

where

$$R_1 = \sqrt{\left[x^2 - a^2 - \alpha^2\epsilon^2(y^2 - a^2)\right]^2 + 4\alpha^2\epsilon^2x^2y^2} \tag{55}$$

$$\Psi_1 = \tan^{-1} \frac{2\alpha\epsilon\ xy}{R_1 + x^2 - a^2 - \alpha^2\epsilon^2 (y^2 - a^2)} \quad . \tag{56}$$

Then

$$\frac{1}{z_1 + w_1'} = \frac{x - \sqrt{R_1}\ \cos \Psi_1 + i(\alpha\epsilon y - \sqrt{R_1}\ \sin \Psi_2)}{a^2 (1 - \alpha^2\epsilon^2)} \quad . \tag{57}$$

Similarly

$$\frac{1}{z_2 + w_2'} = \frac{x - \sqrt{R_2}\ \cos \Psi_2 + i(\beta\epsilon y - \sqrt{R_2}\ \sin \Psi_2)}{a^2 (1 - \beta^2\epsilon^2)} \tag{58}$$

where

$$R_2 = \sqrt{\left[x^2 - a^2 - \beta^2\epsilon^2 (y^2 - a^2)\right]^2 + 4\beta^2\epsilon^2 x^2 y^2} \quad . \tag{59}$$

$$\Psi_2 = \tan^{-1} \frac{2\beta\epsilon\ xy}{R_2 + x^2 - a^2 - \beta^2\epsilon^2 (y^2 - a^2)} \quad . \tag{60}$$

To keep the displacements single-valued, $\underline{\Psi_1}$ and $\underline{\Psi_2}$ must always be taken so that the following relations hold:

$$\left| z_1 + w_1' \right| \geqq \left| a \sqrt{1 - \alpha^2\epsilon^2} \right|$$

$$\left| z_2 + w_2' \right| \geqq \left| a \sqrt{1 - \beta^2\epsilon^2} \right| \quad .$$

Taking the real parts, equations (53) become

$$u = \frac{S}{(\alpha - \beta)\, E_x} \left[\left(\epsilon\alpha^2 + \frac{\sigma_{xy}}{\epsilon}\right) \frac{\left(x - \sqrt{R_1}\, \cos \Psi_1\right)}{1 - \alpha\epsilon} - \left(\epsilon\beta^2 + \frac{\sigma_{xy}}{\epsilon}\right) \frac{\left(x - \sqrt{R_2}\, \cos \Psi_2\right)}{1 - \beta\epsilon} \right] + \frac{Sx}{E_x} \tag{61}$$

$$v = \frac{S}{(\alpha - \beta)\, E_y} \left[- \left(\frac{1}{\epsilon} + \epsilon\alpha^2 \sigma_{yx}\right) \frac{\left(\alpha\epsilon y - \sqrt{R_1}\, \sin \Psi_1\right)}{\alpha\epsilon\,(1 - \alpha\epsilon)} + \left(\frac{1}{\epsilon} + \epsilon\beta^2 \sigma_{yx}\right) \frac{\left(\beta\epsilon y - \sqrt{R_2}\, \sin \Psi_2\right)}{\beta\epsilon\,(1 - \beta\epsilon)} \right] - \frac{S\sigma_{yx}}{E_y}\, y \quad . \tag{62}$$

These equations for the displacements would be used to check data given by strain gages of finite length, since the strains computed from the gage readings are average strains.

Isotropic Stress Function as the Limiting Case of the Orthotropic Stress Function

It is of interest to obtain from (16) the stress function for the corresponding problem when $\frac{b}{a} = 1$ for an isotropic material.

Substituting from (15) and (30), (16) becomes

$$F = R\left\{\frac{Sb}{2\epsilon\left(e^{\phi/2} - e^{-\phi/2}\right)}\left[-\frac{1}{a - e^{\phi/2}\,\epsilon b}\left(\frac{1}{2}(z_1 - w_1)^2 + \gamma_1^2 \log(z_1 + w_1)\right)\right.\right.$$

$$\left.\left. + \frac{1}{a - e^{-\phi/2}\,\epsilon b}\left(\frac{1}{2}(z_2 - w_2)^2 + \gamma_2^2 \log(z_2 + w_2)\right)\right]\right\} + \frac{S\eta^2}{2\epsilon^2} \tag{63}$$

For an isotropic material ϕ becomes equal to 0, and α, β, and ε each becomes equal to unity as shown by equations (6), (8), (11), and (15). For these values, parts of equation (63) take the indeterminate form $\frac{0}{0}$. Evaluating by differentiating both numerator and denominator with respect to ϕ (remembering that z_1, x_2, γ_1, and γ_2 all contain ϕ), It follows that

$$
\begin{aligned}
F = \lim_{\phi \to 0} \Bigg\{ R \Bigg\{ & \frac{Sb}{\epsilon(e^{\phi/2} + e^{-\phi/2})} \Bigg[- \frac{1}{a - e^{\phi/2}\epsilon b} \Bigg(\frac{(z_1 - w_1)}{2} \Big(ie^{\phi/2}\eta - \frac{z_1 ie^{\phi/2}\eta + e^{\phi}\epsilon^2 b^2}{w_1} \Big) \\
& + \frac{\gamma_1^2}{2} \frac{ie^{\phi/2}\eta + \dfrac{z_1 ie^{\phi/2}\eta + e^{\phi}\epsilon^2 b^2}{w_1}}{z_1 + w_1} - e^{\phi}\epsilon^2 b^2 \log(z_1 + w_1) \Bigg) - \frac{e^{\phi/2}\epsilon b}{2(a - e^{\phi/2}\epsilon b)^2} \\
& \times \Bigg(\frac{1}{2}(z_1 - w_1)^2 + \gamma_1^2 \log(z_1 + w_1) \Bigg) + \frac{1}{a - e^{-\phi/2}\epsilon b} \Bigg(\frac{(z_2 - w_2)}{2} \Big(-ie^{-\phi/2}\eta \\
& + \frac{z_2 ie^{-\phi/2}\eta + e^{-\phi}\epsilon^2 b^2}{w_2} \Big) + \frac{\gamma_2^2}{2} \frac{-ie^{-\phi/2}\eta - \dfrac{z_2 ie^{-\phi/2}\eta + e^{-\phi}\epsilon^2 b^2}{w_2}}{z_2 + w_2} + e^{-\phi}\epsilon^2 b^2 \log(z_2 + w_2) \Bigg) \\
& - \frac{e^{-\phi/2}\epsilon b}{2(a - e^{-\phi/2}\epsilon b)^2} \Bigg(\frac{1}{2}(z_2 - w_2)^2 + \gamma_2^2 \log(z_2 + w_2) \Bigg) \Bigg] \Bigg\} \Bigg] \Bigg\} + \frac{S\eta^2}{2\epsilon^2}
\end{aligned}
\tag{64}
$$

Let $\underline{\phi} = 0$ and $\underline{\varepsilon} = 1$. Then (64) takes the form

$$F = R\left\{\frac{Sb}{2}\left[-\frac{1}{a-b}\left((z-w)\left(\frac{iyw - iyz - b^2}{w}\right)\right) - \frac{b}{2(a-b)^2}(z-w)^2\right.\right.$$

$$\left.\left. - \frac{a+b}{w}\left(iy + \frac{b^2}{z+w}\right) - b\log(z+w) + \frac{y^2}{b}\right]\right\} \tag{65}$$

where

$$w = \sqrt{z^2 - a^2 + b^2}$$

On setting $\underline{b} = \underline{a}$, parts of equation (65) assume the indeterminate form $\frac{0}{0}$. On evaluating (65), it is found that for the circular hole,

$$F = R\left\{\frac{Sa}{2}\left[\frac{a^3}{z^2} - \frac{a^3}{2z^2} - \frac{2aiy}{z} - \frac{a^3}{z^2} - a\log 2z + \frac{y^2}{a}\right]\right\} \tag{66}$$

$$= R\left\{\frac{S}{4}\left[-\frac{a^4}{z^2} - \frac{4a^2iy}{z} + 2y^2 - 2a^2\log z - 2a^2\ \ln 2\right]\right\} \tag{67}$$

Since the constant $\underline{2a^2 \log 2}$ will not appear in the stresses obtained from (67), it may be omitted. The real. part of (67) is in polar form:

$$F = \frac{S}{4}\left[-\frac{a^4}{r^2}\cos 2\theta - 4a^2\sin^2\theta + 2r^2\sin^2\theta - 2a^2\log r\right]$$

$$= \frac{S}{4}\left[r^2 - 2a^2\log r - \frac{(r^2 - a^2)^2}{r^2}\cos 2\theta\right] \tag{68}$$

which is the well-known form for the stress function in the corresponding problem for the isotropic plate.[3]

The Effect of Elliptic or Circular Holes on the Stress Distribution in a Plywood Plate

A plywood panel having the grain direction of each ply perpendicular to that of the adjacent plies and having a symmetrical construction may be considered as an orthotropic plate. The strains in such plywood may be obtained from the average stresses (to be defined later), or the average stresses from the strains,[4] by exactly the same relations as exist between the strains and stresses for an orthotropic plate if the apparent elastic moduli of the plywood are used as the elastic moduli of the orthotropic plate. The panel is assumed to remain flat under the application of the loading considered.

The x-axis will be taken parallel to the grain direction of the face plies. The subscript 1 will be used to denote quantities associated with plies having grain direction parallel to the x-axis, and the subscript 2 will be used to denote quantities associated with plies having grain direction parallel to the y-axis.

Let h_1 denote the total thickness of all plies having grain direction parallel to the x-axis.

Let h_2 denote the total thickness of all plies having grain direction parallel to the y-axis,

For plies having grain direction parallel to the x-axis, the following relations hold

$$
\begin{aligned}
(e_{xx})_1 &= \frac{1}{(E_x)_1}\left[(X_x)_1 - (\sigma_{xy})_1 (Y_y)_1\right] \\
(e_{yy})_1 &= \frac{1}{(E_y)_1}\left[(Y_y)_1 - (\sigma_{yx})_1 (X_x)_1\right]
\end{aligned}
\tag{69}
$$

and for plies having grain direction parallel to the y-axis corrosponding equations hold if the subscripts are changed.

Since the panel remains flat, it will be assumed that $\underline{(e_{xx})_1} = \underline{(e_{xx})_2}$. $\underline{(e_{yy})_1} = \underline{(e_{yy})_2}$, $\underline{(e_{xy})_1} = \underline{(e_{xy})_2}$, and it is no longer necessary to write the strain components with subscripts.

Solving equations (69) for the stress components gives

$$(X_x)_1 = \frac{(E_x)_1}{\lambda}\left[e_{xx} + (\sigma_{yx})_1\, e_{yy}\right]$$

$$(Y_y)_1 = \frac{(E_y)_1}{\lambda}\left[e_{yy} + (\sigma_{xy})_1\, e_{xx}\right] \tag{70}$$

where

$$\lambda = 1 - (\sigma_{xy})_1\,(\sigma_{yx})_1$$

Similar relations hold in the remaining plies if the subscripts are changed throughout.

Assuming the plies are all rotary cut and from the choice of axes, the elastic constants have the following values in the respective plies:

$$(E_x)_1 = E_L \qquad (E_x)_2 = E_T$$

$$(E_y)_1 = E_T \qquad (E_y)_2 = E_L$$

$$(\sigma_{xy})_1 = \sigma_{LT} \qquad (\sigma_{xy})_2 = \sigma_{TL}$$

$$(\sigma_{yx})_1 = \sigma_{TL} \qquad (\sigma_{yx})_2 = \sigma_{LT} \quad .$$

After making these changes, equations (70) become

$$\begin{aligned}
(X_x)_1 &= \frac{E_L}{\lambda}\left[e_{xx} + \sigma_{TL}\, e_{yy}\right] \\
(Y_y)_1 &= \frac{E_T}{\lambda}\left[e_{yy} + \sigma_{LT}\, e_{xx}\right] \\
(X_x)_2 &= \frac{E_T}{\lambda}\left[e_{xx} + \sigma_{LT}\, e_{yy}\right] \\
(Y_y)_2 &= \frac{E_L}{\lambda}\left[e_{yy} + \sigma_{TL}\, e_{xx}\right]
\end{aligned} \tag{71}$$

where

$$\lambda = 1 - \sigma_{TL}\, \sigma_{LT} \quad .$$

It is now important to define the mean stress components $\overline{X}_x$ and $\overline{Y}_y$ by the following equations:

$$\overline{X}_x = \frac{h_1 (X_x)_1 + h_2 (X_x)_2}{h} = \frac{h_1 E_L + h_2 E_T}{h\lambda} e_{xx} + \frac{\sigma_{TL} E_L}{\lambda} e_{yy}$$

$$\overline{Y}_y = \frac{h_1 (Y_y)_1 + h_2 (Y_y)_2}{h} = \frac{h_1 E_T + h_2 E_L}{h\lambda} e_{yy} + \frac{\sigma_{TL} E_L}{\lambda} e_{xx} \tag{72}$$

where $h = h_1 + h_2$, the overall thickness of the plywood, and the relation

$$\frac{\sigma_{LT}}{E_L} = \frac{\sigma_{TL}}{E_T}$$

ham been used.

Equations (72) may be rewritten as follows:

$$\overline{X}_x = \frac{E_a}{\lambda} \left[e_{xx} + \overline{\sigma}_{yx} e_{yy} \right]$$

$$\overline{Y}_y = \frac{E_b}{\lambda} \left[e_{yy} + \overline{\sigma}_{xy} e_{xx} \right] \tag{73}$$

where

$$E_a = \frac{h_1 E_L + h_2 E_T}{h} \qquad E_b = \frac{h_1 E_T + h_2 E_L}{h}$$

$$\overline{\sigma}_{xy} = \frac{\sigma_{TL} E_L}{E_b} \qquad \overline{\sigma}_{yx} = \frac{\sigma_{TL} E_L}{E_a} \tag{74}$$

Solving equations (73) for the strain components gives

$$e_{xx} = \frac{\lambda}{(1 - \bar{\sigma}_{xy}\,\bar{\sigma}_{yx})}\,\frac{1}{E_a}\left[\bar{X}_x - \bar{\sigma}_{xy}\,\bar{Y}_y\right]$$

$$e_{yy} = \frac{\lambda}{(1 - \bar{\sigma}_{xy}\,\bar{\sigma}_{yx})}\,\frac{1}{E_b}\left[\bar{Y}_y - \bar{\sigma}_{yx}\,\bar{X}_x\right]$$

or

$$e_{xx} = \frac{1}{\bar{E}_x}\left[\bar{X}_x - \bar{\sigma}_{xy}\,\bar{Y}_y\right]$$

$$e_{yy} = \frac{1}{\bar{E}_y}\left[\bar{Y}_y - \bar{\sigma}_{yx}\,\bar{X}_x\right] \tag{75}$$

where [7]

$$\bar{E}_x = \frac{E_a\,(1 - \bar{\sigma}_{xy}\,\bar{\sigma}_{yx})}{\lambda}$$

$$\bar{E}_y = \frac{E_b\,(1 - \bar{\sigma}_{xy}\,\bar{\sigma}_{yx})}{\lambda} \tag{76}$$

It is easily established that $\dfrac{\bar{\sigma}_{xy}}{\bar{E}_x} = \dfrac{\bar{\sigma}_{yx}}{\bar{E}_y}$

---

[7] Since σ_{xy}, $\bar{\sigma}_{xy}$, etc. are usually small, $\bar{E}_x$ and $\bar{E}_y$ are approximately equal to E_a and E_b, respectively.

In plies with grain direction parallel to the x-axis, the conditions of equilibrium require

$$\frac{\partial(X_x)_1}{\partial x} + \frac{\partial(X_y)_1}{\partial y} = 0$$

$$\frac{\partial(X_y)_1}{\partial x} + \frac{\partial(Y_y)_1}{\partial y} = 0$$

and similarly in the remaining plies

$$\frac{\partial(X_x)_2}{\partial x} + \frac{\partial(X_y)_2}{\partial y} = 0$$

$$\frac{\partial(X_y)_2}{\partial x} + \frac{\partial(Y_y)_2}{\partial y} = 0 \quad .$$

Then

$$h_1 \frac{\partial(X_x)_1}{\partial x} + h_1 \frac{\partial(X_y)_1}{\partial y} = 0 \tag{77}$$

$$h_1 \frac{\partial(X_y)_1}{\partial x} + h_1 \frac{\partial(Y_y)_1}{\partial y} = 0 \tag{78}$$

and

$$h_2 \frac{\partial(X_x)_2}{\partial x} + h_2 \frac{\partial(X_y)_2}{\partial y} = 0 \tag{79}$$

$$h_2 \frac{\partial(X_y)_2}{\partial x} + h_2 \frac{\partial(Y_y)_2}{\partial y} = 0 \quad . \tag{80}$$

Adding equations (77) and (79) and dividing by $\underline{h}$, it is found that

$$\frac{\partial \overline{X}_x}{\partial x} + \frac{\partial \overline{X}_y}{\partial y} = 0 \tag{81}$$

where, since in all plies the relation

$$X_y = \mu_{LT}\, e_{xy}$$

holds, the mean stress component $\underline{\overline{X}_y}$ is identical with the stress component $\underline{X_y}$.

Similarly equation (78) and (80) yield

$$\frac{\partial \overline{X}_y}{\partial x} + \frac{\partial \overline{Y}_y}{\partial y} = 0 \tag{82}$$

Equations (81) and (82) will be satisfied by a stress function $\underline{F}$, such that

$$\overline{X}_x = \frac{\partial^2 F}{\partial y^2} \ , \qquad \overline{Y}_y = \frac{\partial^2 F}{\partial x^2} \ , \qquad \overline{X}_y = -\frac{\partial^2 F}{\partial x \partial y} \quad . \tag{83}$$

Substituting (83) in (75) and then making use of the compatibility equation

$$\frac{\partial^2 e_{xx}}{\partial y^2} + \frac{\partial^2 e_{yy}}{\partial x^2} = \frac{\partial^2 e_{xy}}{\partial x \partial y}$$

the following differential equation satisfied by the stress function F is found:

$$\frac{1}{\overline{E}_y}\frac{\partial^4 F}{\partial x^4} + \left[\frac{1}{\mu_{LT}} - \frac{2\overline{\sigma}_{xy}}{\overline{E}_x}\right]\frac{\partial^4 F}{\partial x^2 \partial y^2} + \frac{1}{\overline{E}_y}\frac{\partial^4 F}{\partial y^4} = 0 \quad .$$

As in the treatment of equation (3), it will be convenient to rewrite this equation as

$$\frac{\partial^4 F}{\partial x^4} + 2\kappa\frac{\partial^4 F}{\partial x^2 \partial \eta^2} + \frac{\partial^4 F}{\partial \eta^4} = 0 \tag{84}$$

where

$$\kappa = \frac{\sqrt{\overline{E}_x \overline{E}_y}}{2}\left(\frac{1}{\mu_{LT}} - \frac{2\overline{\sigma}_{xy}}{\overline{E}_x}\right) \tag{85}$$

by making the substitution

$$\eta = \epsilon y \tag{86}$$

where

$$\epsilon = \sqrt[4]{\frac{\overline{E}_x}{\overline{E}_y}} \tag{87}$$

The differential equations (84) and (5) are of the same form mathematically, and any solution of (5) is a solution of (84) if the appropriate constants are used. It is then possible by using equations (31), (32), and (33) to obtain the stress distribution in the neighborhood of an elliptic hole situated in the middle of a plywood plate subjected to a uniform tension, provided that the axes of the ellipse are parallel and perpendicular to the grain of the face plies and that the tension is applied parallel or perpendicular to the axes of the ellipse.

Hence, if the $\underline{K}$ and $\underline{\varepsilon}$ calculated from the apparent clastic: moduli of plywood are used, all of the preceding discussion for orthotropic plates containing elliptic holes holds for plywood panels.

Numerical values for the stresses at various points along the $\underline{x}$- and $\underline{y}$-axes in the case $\frac{b}{a} = 1$ for rotary-cut Sitka spruce plywood having half the material with grain direction parallel to the $\underline{x}$-axis are given in tables 6 and 7. Figures 10, 11, 12, and 13 illustrate how these stresses vary in the neighborhood of the hole.

The foregoing analysis for plywood is based on the assumption that all plies are rotary cut and of the same species of wood. When these assumptions are not fulfilled, it is easy to make suitable modifications in the analysis (see appendix).

Appendix

A plain-sawn or a quarter-sawn wood plate ox a plywood plate may be considered to have two perpendicular axes of elastic symmetry in the plane of the plate. The discussion given in this appendix applies to a rectangular plate of this type with its edges parallel to the axes of symmetry and with a small circular hole at the center. The x- and y-axes are taken as the axes of symmetry. A uniform tension S directed parallel to the x-axis is supposed to act on the two opposite edges of the plate, and the tensile stress on the edge of the hole at the end of the diameter perpendicular to the uniform tension is given by

$$S\,(\alpha\epsilon + \beta\epsilon + 1) \quad .$$

For wood, the constants that appear in this expression are defined a3 follows:

$$\varepsilon = \sqrt[4]{\frac{E_x}{E_y}}$$

$$\alpha = e^{\phi/2}$$

$$\beta = e^{-\phi/2}$$

e = natural logarithmic base

E_x = Young's modulus in the x-direction

E_y = Young's modulus in the y-direction

$$\phi = \cosh^{-1}\kappa$$

$$\kappa = \frac{\sqrt{E_x E_y}}{2}\left(\frac{1}{\mu_{xy}} - \frac{2\sigma_{xy}}{E_x}\right)$$

μ_{xy} = modulus of rigidity In the xy-plane

σ_{xy} = the Poisson's ratio given by the ratio of the contraction parallel to the y-axis to the extension parallel to the x-axis associated with a tension parallel to the x-axis.

For plywood, equations similar to those already given for wood define ε, α, β, ϕ, and κ if the remaining constants are as subsequently defined.

The plies will be considered to be numbered consecutively from the upper to the lower face. The elastic moduli in the ith ply will be denoted by $(E_x)_i$, $(E_y)_i$, $(\mu_{xy})_i$, and $(\sigma_{xy})_i$. The thickness of the ith ply is h_i. That of the plate is h.

Then approximately[4]

$$E_x = E_a = \frac{\Sigma (E_x)_i h_i}{h}$$

$$E_y = E_b = \frac{\Sigma (E_y)_i h_i}{h}$$

$$\mu_{xy} = \frac{\Sigma (\mu_{xy})_i h_i}{h}$$

$$\sigma_{xy} = \frac{\Sigma h_i (E_y)_i (\sigma_{xy})_i}{h E_b}$$

The shear parallel or perpendicular to direction of the uniform tension and on the edge of the circular hole is given in the mathematical part of the report by equation (43) if b is set equal to a. By substituting the constants defined previously, this shear stress may be plotted as a function of the polar coordinate θ (fig. 5), and its maximum value read from the curve.

Table 1. --Elastic moduli of Sitka spruce and yellow popular[1]

Species	E_L	E_T	E_R	μ_{LT}	μ_{LR}	σ_{LT}	σ_{LR}
	1,000 lb. per sq. in.						
Sitka spruce	1,679	76	(2)	112	(2)	0.464	(2)
Yellow-poplar	1,775	(2)	130	(2)	113.6	(2)	0.337

[1] The elastic moduli of Sitka spruce are average values obtained from a large number of tests made at the U.S. Forest Products Laboratory. The elastic moduli of yellow-poplar are values obtained from the one specimen used in the experimental verification of this report.

[2] Not used.

Table 2. --Observed and theoretical values of the strains at the points P and Q of figure 3

Type	Strain at P	Strain at Q	Ratio of strain at P to strain at Q
	Inch per inch		
Observed	12.3×10^{-4}	2.75×10^{-4}	4.47
Theoretical (computed from equations (35) and (45b))	3.22×10^{-6} S	0.603×10^{-6} S	5.34

Table 3. --Values of the shear component X_y on the edge of a circular hole for a plain-sawn plate of Sitka spruce

θ	0°	5°	10°	15°	20°	25°	30°	35°	40°	45°
$\frac{X_y}{S}$	0	0.0183	0.0354	0.0496	0.0596	0.0635	0.0591	0.0440	0.0151	-0.0308

θ	50°	55°	60°	65°	70°	75°	78°	80°	85°	90°
$\frac{X_y}{S}$	-0.0973	-0.1877	-0.3033	-0.4407	-0.5846	-0.6948	-0.7123	-0.6888	-0.4582	0

Table 4. --Values of the stress components at points along the x-axis exterior to a circle of radius a and with center at the origin for a plain-sawn plate of Sitka spruce.

x	$\frac{X_x}{S}$	$\frac{Y_y}{S}$
1.0a	0	-0.2128
1.1a	-0.0157	-0.1762
1.2a	- .0216	- .1458
1.3a	- .0198	- .1205
1.4a	- .0118	- .0993
1.5a	+ .0010	- .0817
1.6a	.0175	- .0669
1.7a	.0368	- .0554
1.8a	.0582	- .0440
1.9a	.0811	- .0352
2.0a	.1050	- .0278
3.0a	.3448	+ .0052
4.0a	.5280	.0106
5.0a	.6530	.0102
6.0a	.7379	.0087
7.0a	.7967	.0073
8.0a	.8384	.0060
9.0a	.8689	.0050
10.0a	.8918	.0042

Table 5.-- Values of the stress components at points along the y-axis exterior to a circle of radius a and with center at the origin for a plain-sawn plate of Sitka spruce

y	$\frac{X_x}{S}$	$\frac{Y_y}{S}$
1.0a	5.8439	0
1.1a	2.7262	0.1566
1.2a	2.0069	.1522
1.3a	1.6871	.1345
1.4a	1.5089	.1171
1.5a	1.3968	.1021
1.6a	1.3205	.0895
1.7a	1.2657	.0790
1.8a	1.2248	.0701
1.9a	1.1932	.0627
2.0a	1.1682	.0564
3.0a	1.0629	.0245
4.0a	1.0335	.0137
5.0a	1.0209	.0087
6.0a	1.0143	.0060
7.0a	1.0104	.0044
8.0a	1.0079	.0034
9.0a	1.0063	.0027
10.0a	1.0050	.0022

Table 6. --Values of the stress components at points along the x-axis exterior to a circle of radius a and with center at the origin for a rotary-cut plywood plate of Sitka spruce

x	$\frac{X_x}{S}$	$\frac{Y_y}{S}$
1.00a	0	-1.0000
1.05a	-0.0223	.....
1.10a	- .0195	- .4324
1.15a	- .0076	.....
1.20a	+ .0085	- .2467
1.25a	+ .0268	- .1934
1.50a	+ .1275	- .0630
2.00a	+ .3130	+ .0062
3.00a	+ .5682	+ .0229
4.00a	+ .7143	+ .0191
5.00a	+ .8005	+ .0146

Table 7. -- values of the stress components at points along the y-axis exterior to a circle of radius a and with center at the origin for a rotary-cut plywood plate of Sitka spruce

y	$\frac{X_x}{S}$	$\frac{Y_y}{S}$
1.0a	4.1335	0
1.2a	2.0108	0.2377
1.3a	1.7417	.2547
1.5a	1.4557	.2583
2.0a	1.2018	.2212
3.0a	1.0733	.1451
4.0a	1.0375	.0973
5.0a	1.0227	.0683

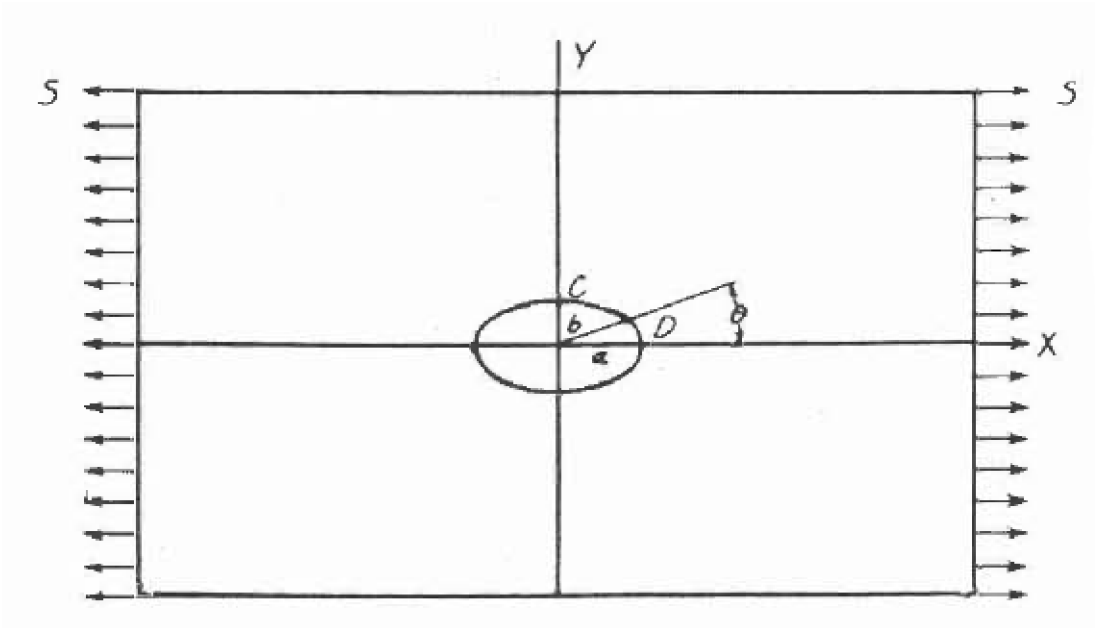

Figure 1--Elliptic hole in orthotropic plate.

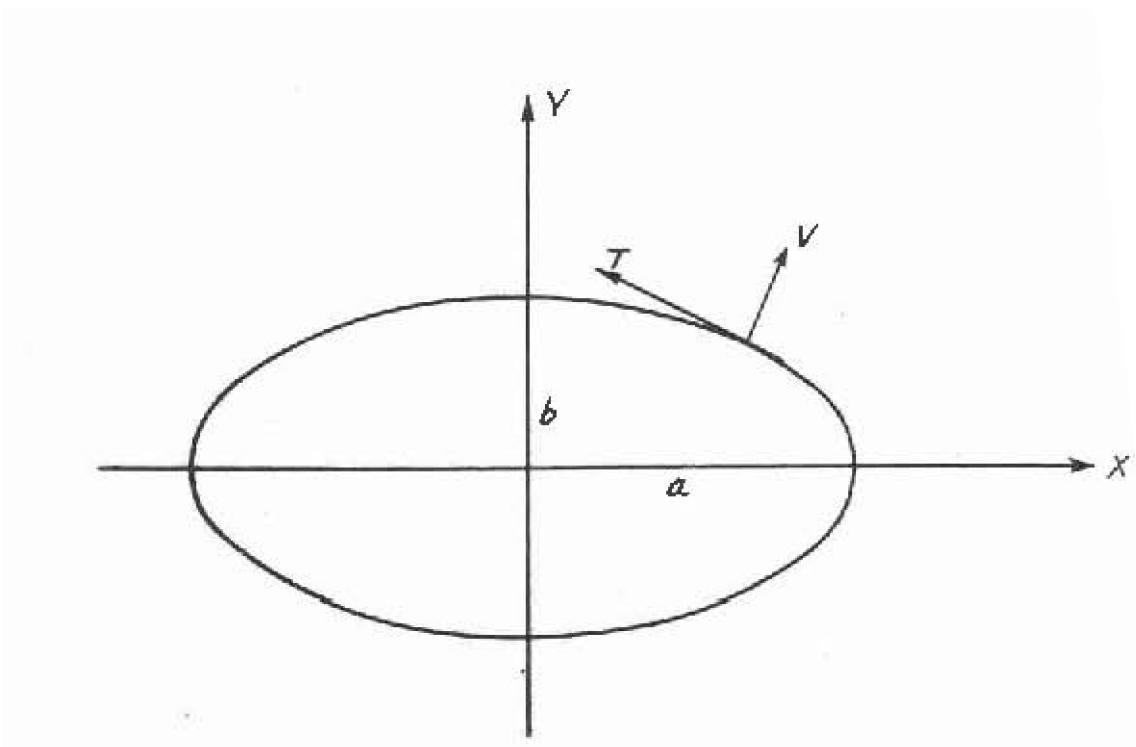

Figure 2.--Orientation of positive normal and tangent on the boundary of the elliptic hole.

Z M 54246 F

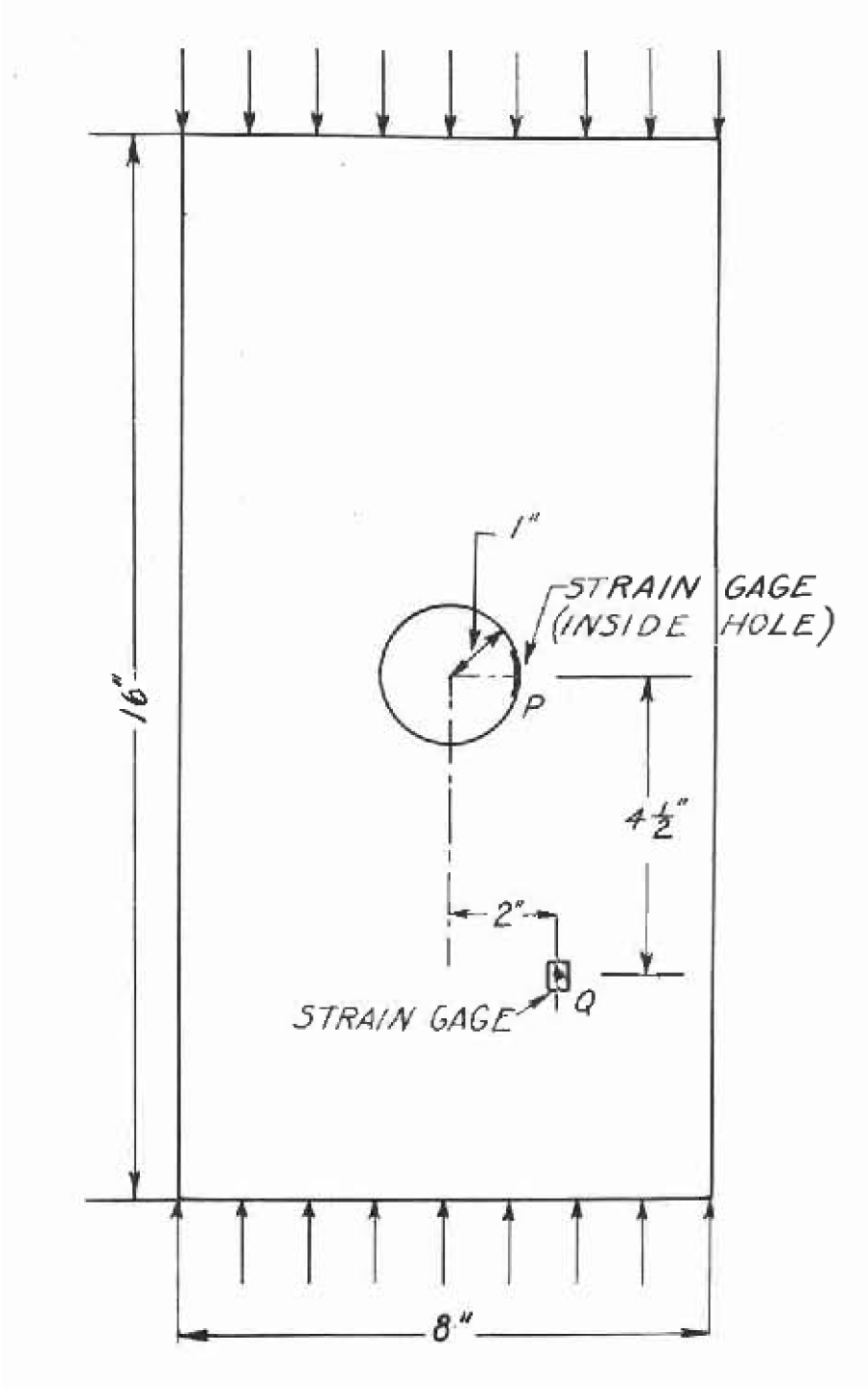

Figure 3.--Circular hole in a quarter-sawn yellow-poplar board subjected to a uniform compression.

Z M 54249 F

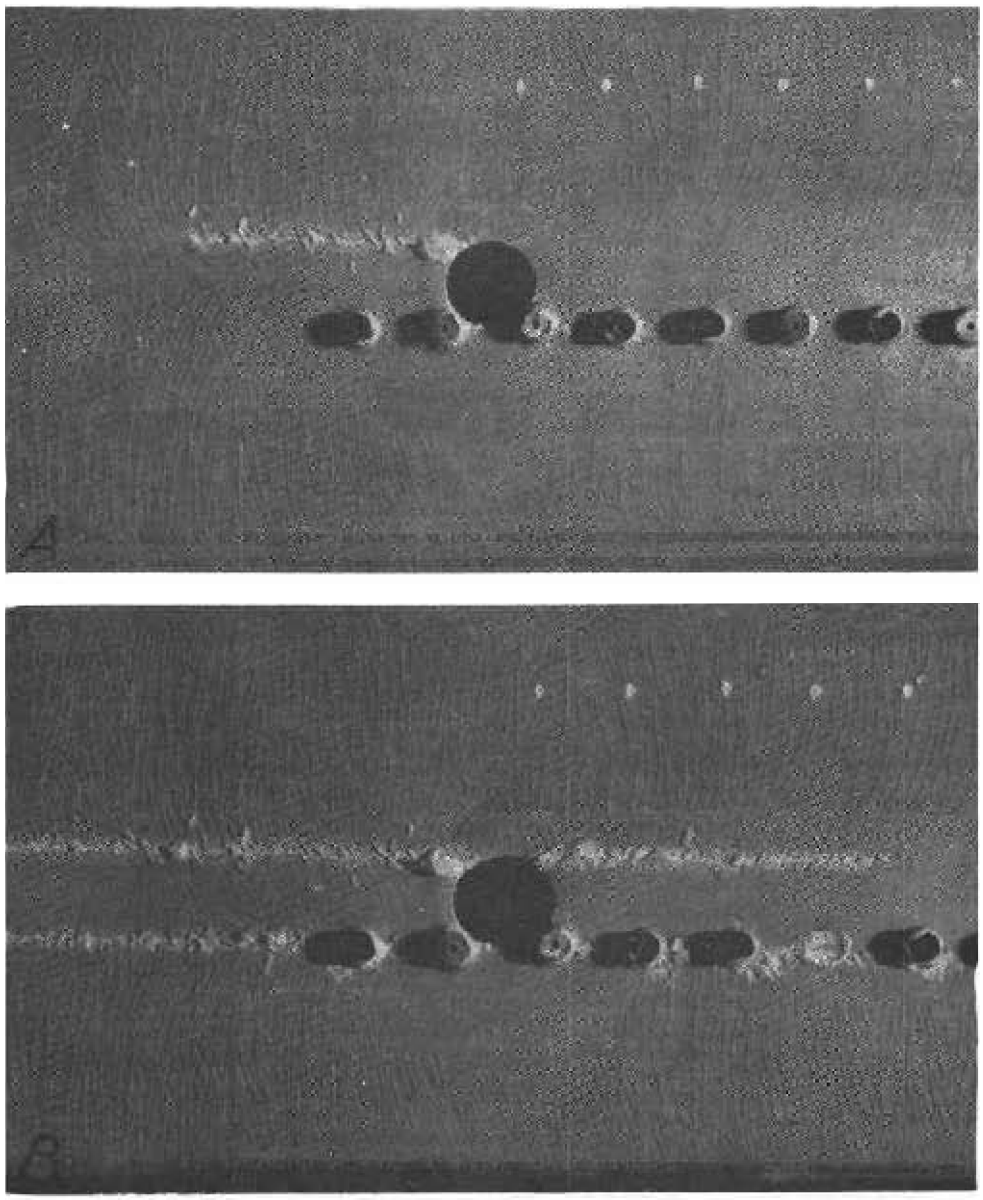

Figure 4.--The tension flange of a loaded wood box beam showing shear failure caused by vertical holes. The beam is subjected to a lower load in A than in B. The small cracks occurred in the stress-coat, which was applied to the beam before testing. The small round objects paralleling the edge of the flange are Whittemore strain gage points.

Z M 54250 F

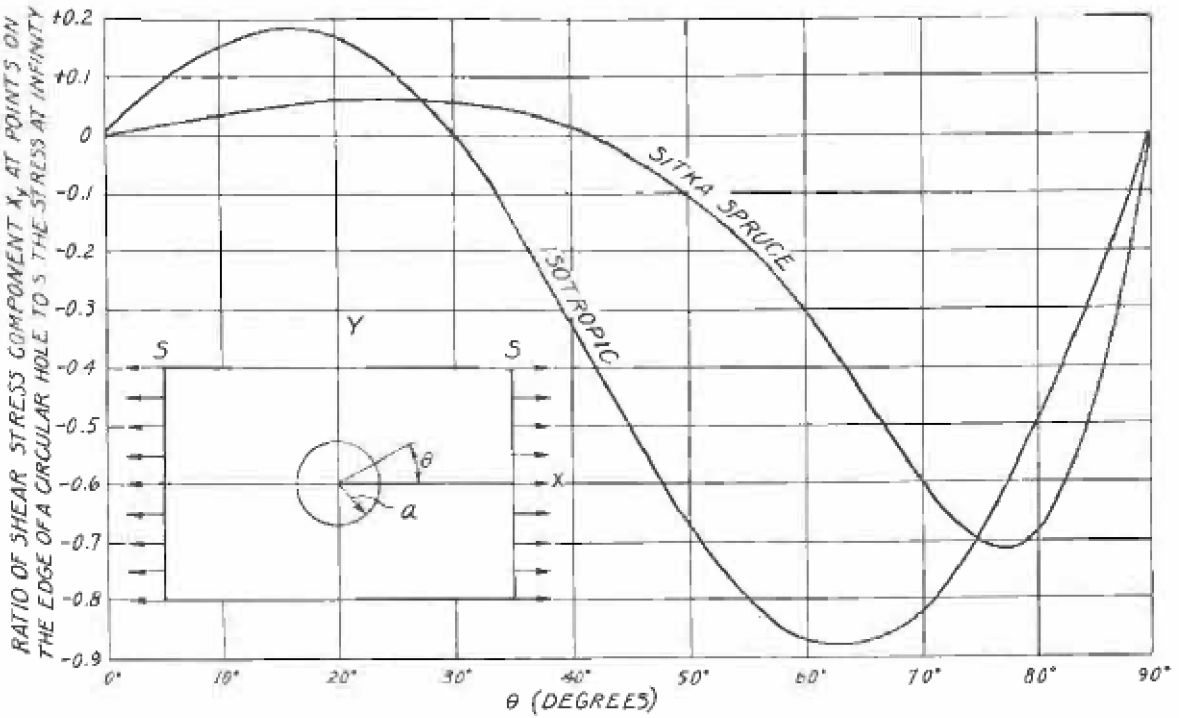

Figure 5.--Variation of the shear stress component X_y around the edge of a circular hole for a plain-sawn plate of Sitka spruce and for an isotropic plate.

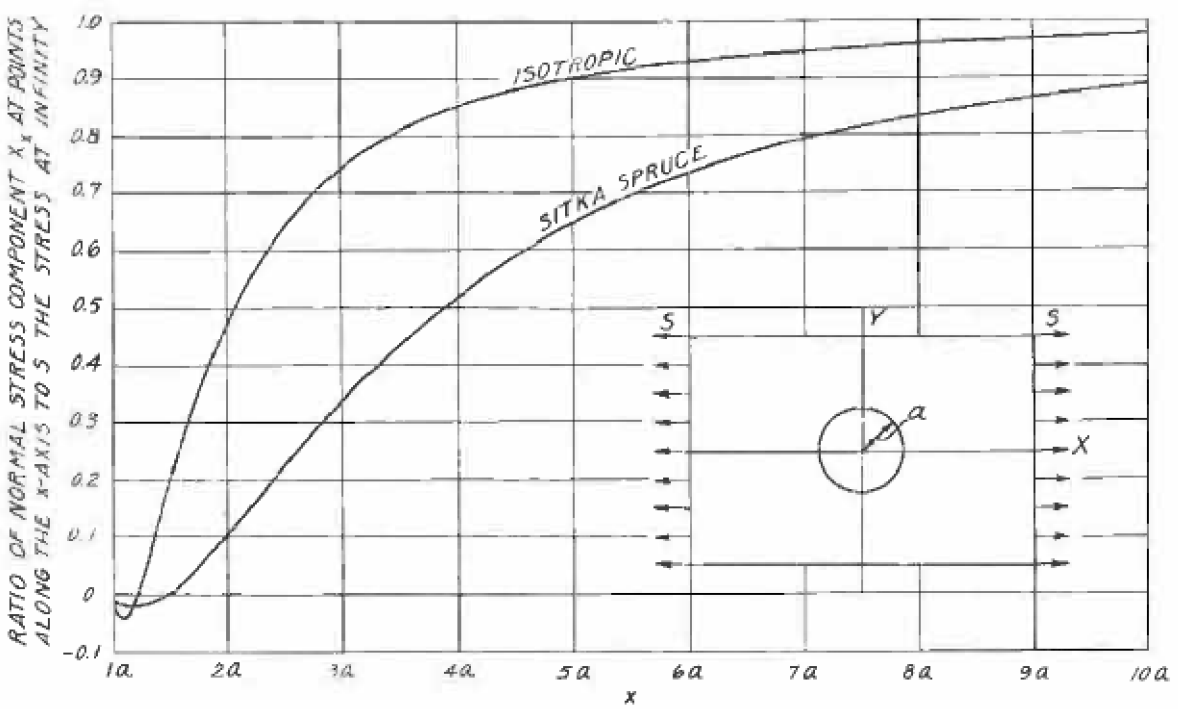

Figure 6.--Variation of the normal stress component χ_x at points along the x-axis exterior to a circular hole of radius a and with center at the origin for a plain-sawn plate of Sitka spruce and for an isotropic plate.

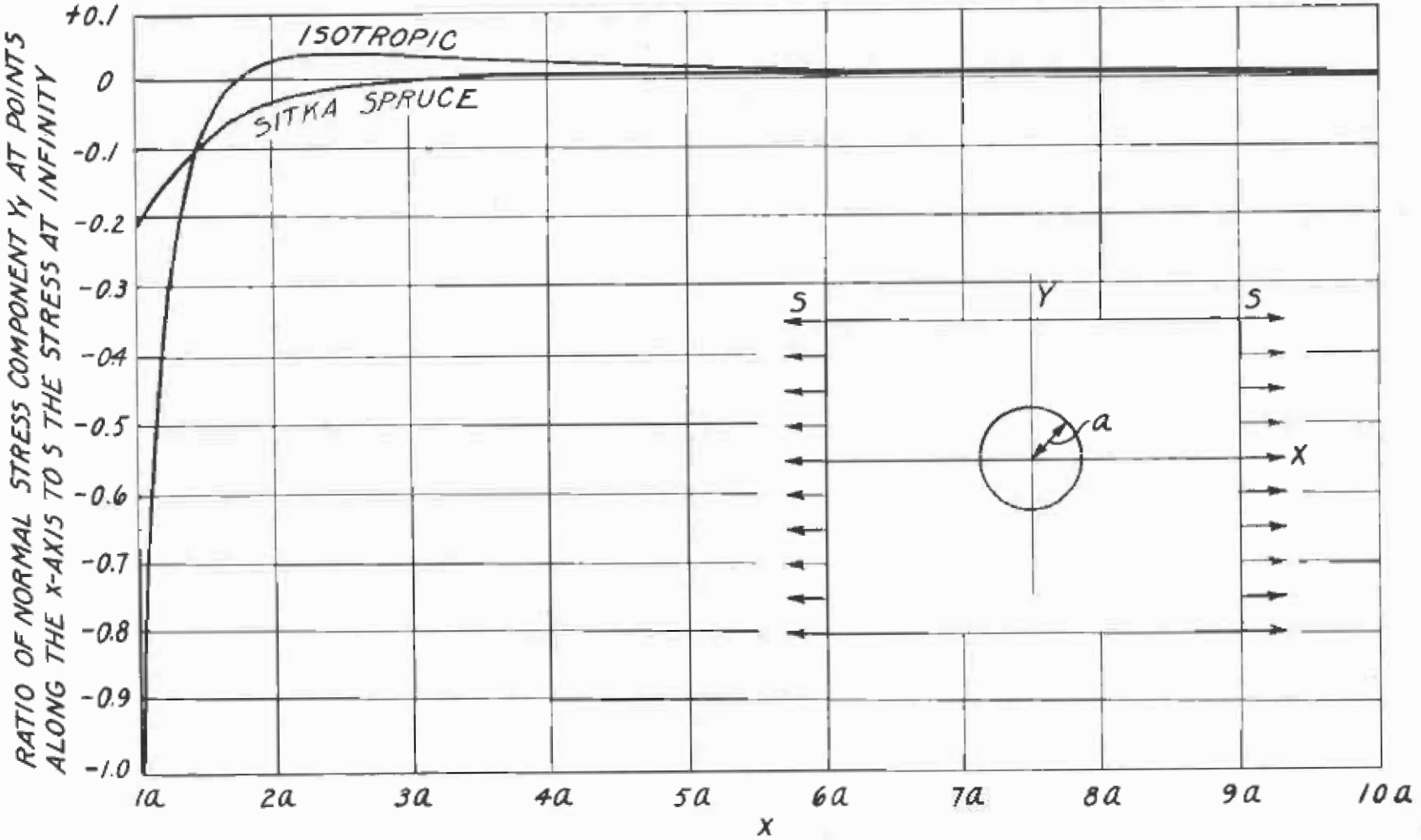

Figure 7.--Variation of the normal stress component Yy at points along the x-axis exterior to a circular hole of radius a and with center at the origin for a plain-sawn plate of Sitka spruce and for an isotropic plate.

ZM 54252 F

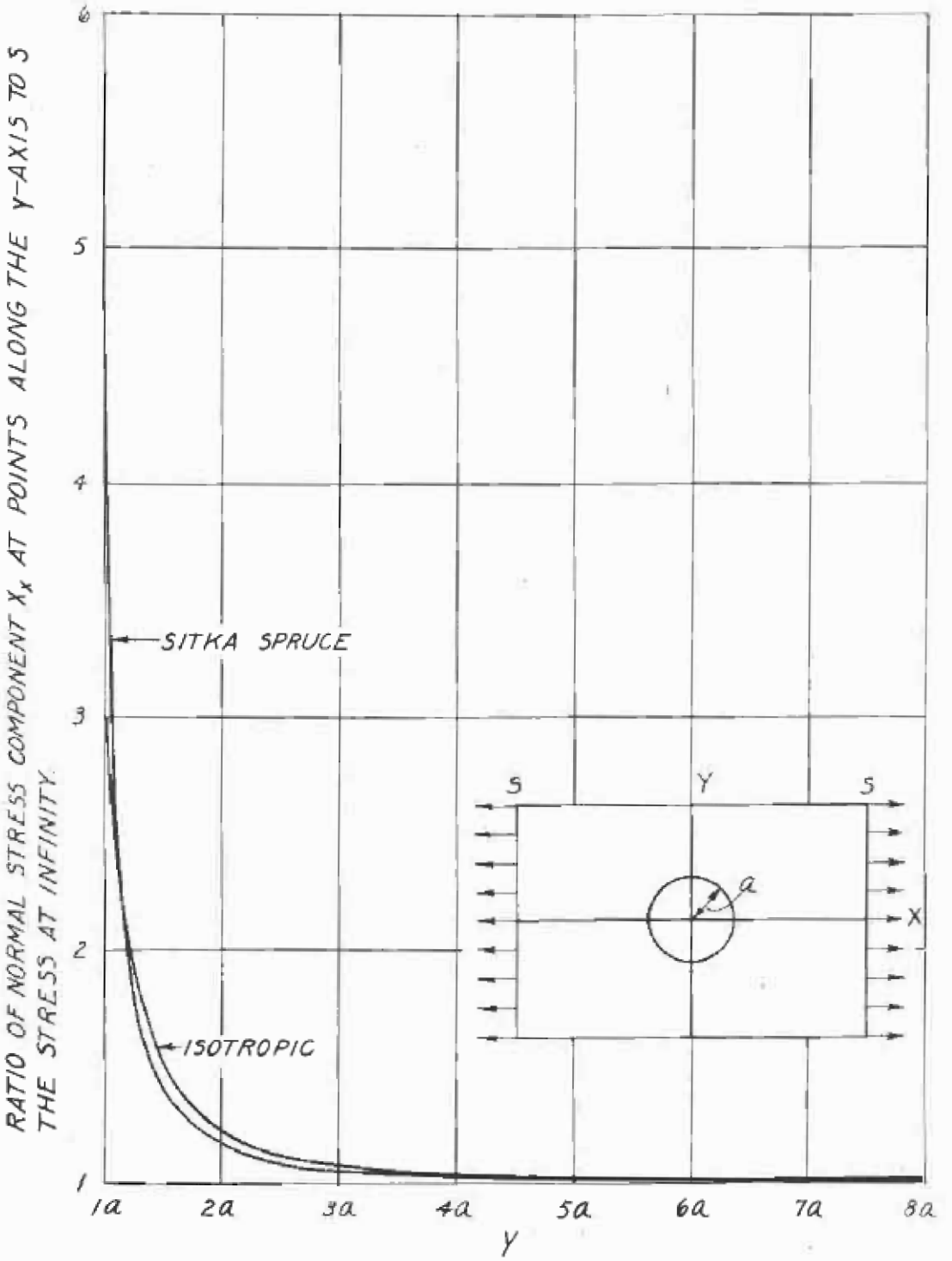

Figure 8.--Variationof the normal stress component X_X at points along the y-axis exterior to a circular hole of radius a and with center at the origin for a plain-sawn plate of Sitka spruce and for an isotropic plate.

Z M 54253 F

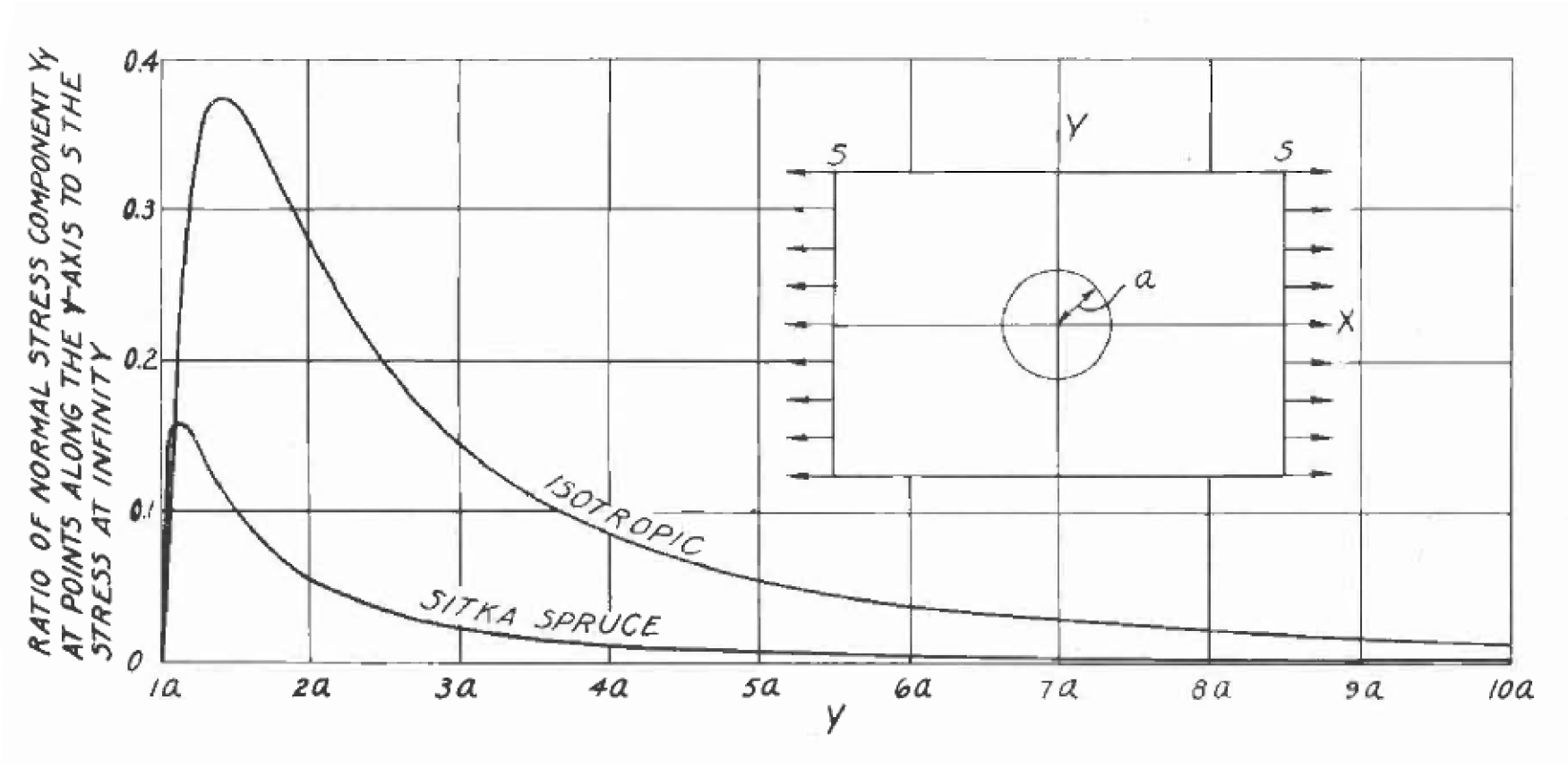

Figure 9.--Variation of the normal stress component Y_y at points along the y-axis exterior to a circular hole of radius a and with center at the origin for a plain-sawn plate of Sitka spruce and for an isotropic plate.

Z M 54254 F

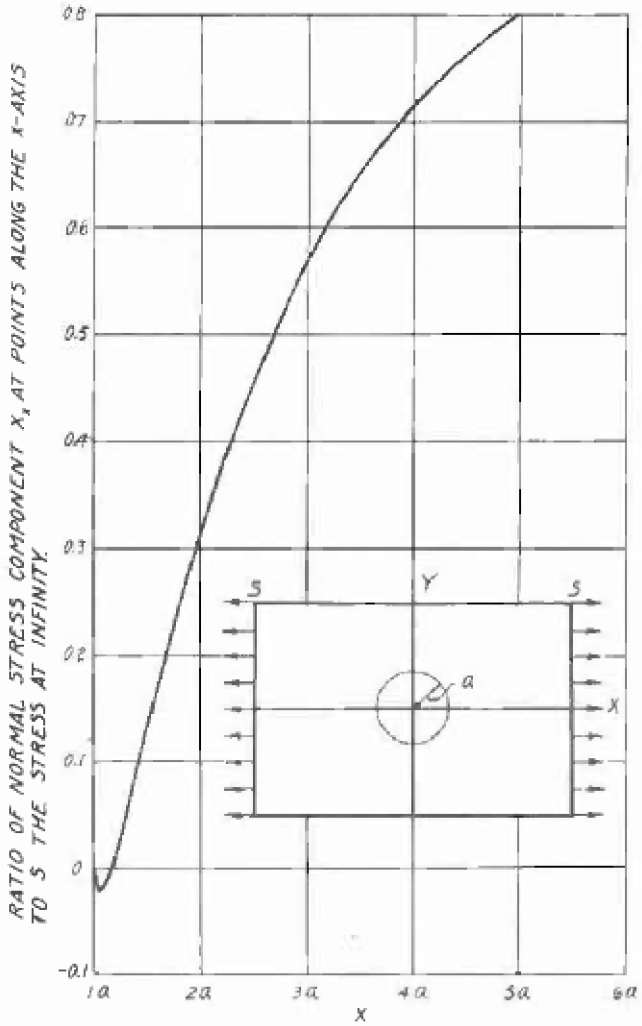

Figure 10.--Variation of the normal stress component Xx at points along the x-axis exterior to a circular hole of radius a with center at the origin for a rotary-cut plywood plate of Sitka spruce

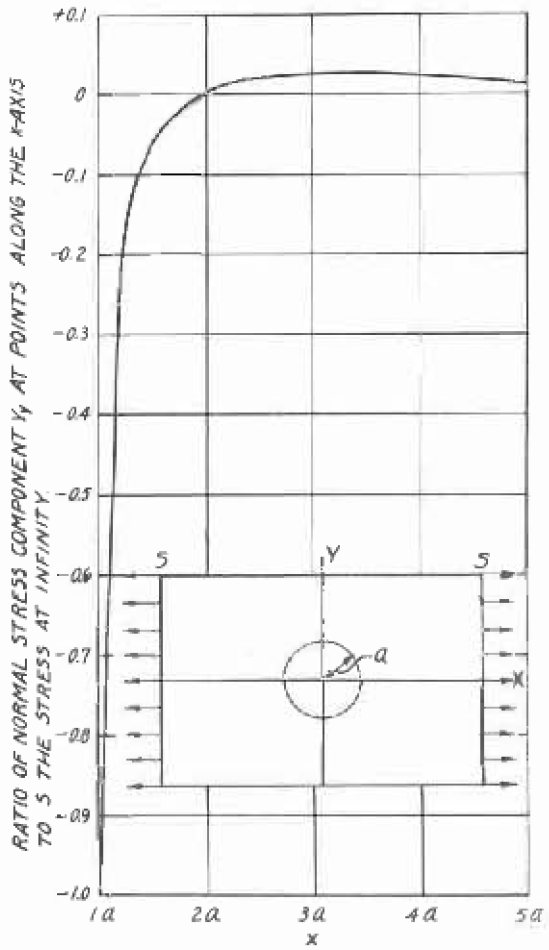

Figure 11.--Variation of the normal stress component Yy at points along the x-axis exterior to a circular hole of radius a and with center at the originfor a rotary-cut plywood plate of Sitka spruce.

Z M 54256 F

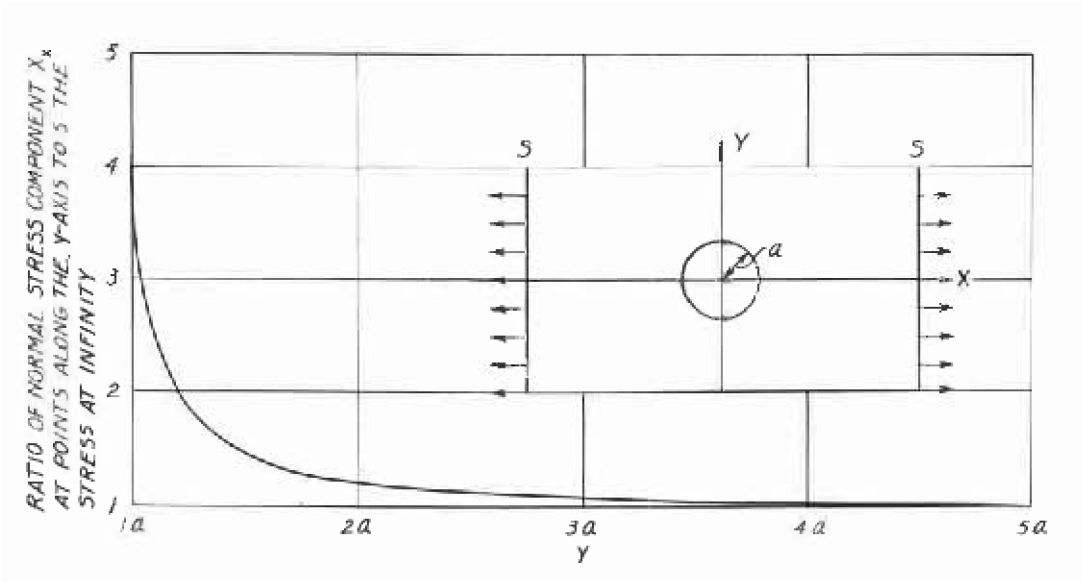

Figure 12.--Variation of the normal stress component X_X at points along the y-axis exterior to a circular hole of radius a and with center at the origin for a rotary-cut plywood plate of Sitka spruce.

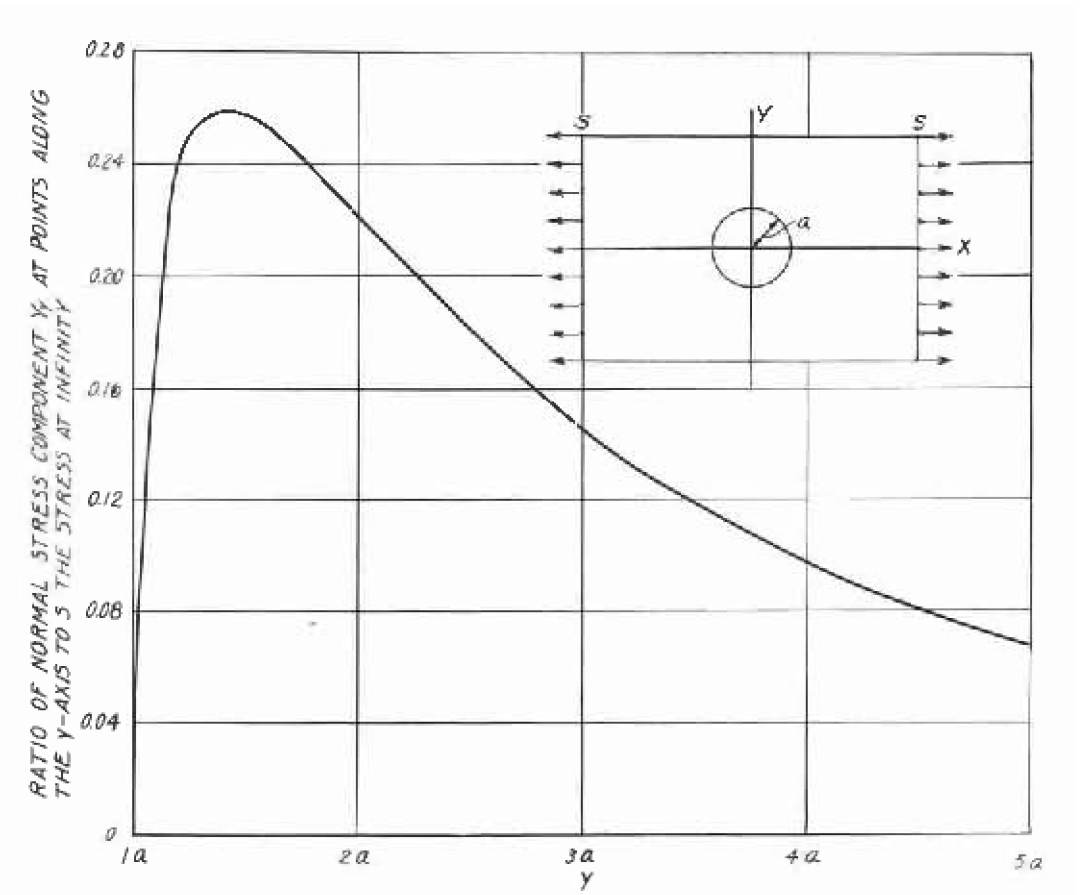

Figure 13.--Variation of the normal stress component Yy at points along the y-axis exterior to a circular hole of radius a and with center at the origin for a rotary-cut plywood plate of Sitka spruce.